Ghost imaging with broad distance*

Duan De-Yang(段德洋)[a], Zhang Lu(张 路)[b], Du Shao-Jiang(杜少将)[c], and Xia Yun-Jie(夏云杰)[a]†

[a] *Shandong Provincial Key Laboratory of Laser Polarization and Information Technology, Research Institute of Laser, Qufu Normal University, Qufu* 273165, *China*

[b] *School of Physical Engineering, Qufu Normal University, Qufu* 273165, *China*

[c] *School of Physics and Information Technology, Jining University, Qufu* 273155, *China*

(Received 13 March 2015; revised manuscript received 5 May 2015; published online 20 August 2015)

We present a scheme that is able to achieve the ghost imaging with broad distance. The physical nature of our scheme is that the different wavelength beams are separated in free space by an optical media according to the slow light or dispersion principle. Meanwhile, the equality of the optical distance of the two light arms is not violated. The photon correlation is achieved by the rotating ground glass plate (RGGP) and spatial light modulator (SLM), respectively. Our work shows that a monochromic ghost image can be obtained in the case of RGGP. More importantly, the position (or distance) of the object can be ascertained by the color of the image. Thus, the imaging and ranging processes are combined as one process for the first time to the best of our knowledge. In the case of SLM, we can obtain a colored image regardless of where the object is.

Keywords: multiwavelength ghost imaging, slow light, dispersion, imaging distance

PACS: 42.30.Va, 42.50.Ar **DOI:** 10.1088/1674-1056/24/10/104203

1. Introduction

Ghost imaging (GI) is a novel imaging technique which has become increasingly popular over the last decade. Probing GI has recently received a lot of interest in view of practical applications, owing to its novel physical characteristics, e.g., GI is a good candidate for imaging objects immersed in optically harsh environments. Early studies include GI in the presence of atmospheric turbulence,[1–3] night vision,[4] and scattering media.[5] In spite of the fact that the physical nature and great progress in application has been studied, GI still seemingly remains in the laboratory research stage. GI is unable to obtain large-scale applications because there are three thorny problems: (i) low image quality [e.g., signal-to-noise ratio (SNR)]; (ii) long computational time; and (iii) the specific plane that the objects must be placed in.

For the first two problems, the researchers conducted in-depth study and proposed many schemes to improve the image quality[6–11] and shorten the computational time.[12–16] For the third problem, three-dimensional (3D) ghost imaging provides a solution.[17–19] According to the slow light or dispersion principle, we propose another imaging scheme that can effectively solve this problem. In this paper, we present the theoretical analysis. Based on the slow light or dispersion principle, the multi-wavelength signal light beams are separated by an optical media in free space. Consequently, although the spatial distance of each monochromatic signal light beam is different, the optical distances are equal to each other. At the same time, they are equal to the idler light beams. Despite the different positions of the object in space, the object still remains in the same optical plane. Thus, the condition of generating GI is not violated.

As we all know, the slow light can be obtained by many methods, e.g., electromagnetically induced transparency (EIT),[20] photonic crystals,[21] and other ways.[22] In this article, we take the EIT as an example to illustrate the broad distance GI. Furthermore, the broad distance GI obtained by dispersion has also been discussed. The photon correlation is achieved by a rotating ground glass plate (RGGP) and spatial light modulator (SLM), respectively. In the case of RGGP, only the degenerate-wavelength photon correlation can be achieved. Thus, a monochromic ghost image can be obtained. Because of this, the position of the object can be ascertained by the color of the ghost image. A colored ghost image can be obtained in the case of SLM because both the degenerate-wavelength and nondegenerate-wavelength photon correlations are obtained by the SLM in general.

2. Analysis

The schematic diagram of our imaging scheme, shown in Fig. 1, is a thermal multi-wavelength lensless GI. In this paper, we utilize two quasi-monochromatic lasers [green (532 nm) and red (770.1 nm)] to expound our work because these two lasers use an effective wave band for the selected EIT system. Two lasers pass through the RGGP and then yield the

*Project supported by the National Natural Science Foundation of China (Grant Nos. 61178012, 11204156, 11304179, and 11247240), the Specialized Research Fund for the Doctoral Program of Higher Education of China (Grant Nos. 20133705110001 and 20123705120002), the Scientific Research Foundation for Outstanding Young Scientists of Shandong Province, China (Grant No. BS2013DX034), and the Natural Science Foundation of Shandong Province, China (Grant No. ZR2012FQ024).

†Corresponding author. E-mail: yjxia@mail.qfnu.edu.cn

© 2015 Chinese Physical Society and IOP Publishing Ltd

idler and signal beams by a 50:50 beam splitter. The idler light beams do not interact with the object but are detected by a charge-coupled device (CCD) camera. However, the signal light beams pass through an optical media first, e.g., $^{40}\mathrm{K}+^{39}\mathrm{K}$ system. Then, they interact with the object and are detected by a bucket detector at last. The output currents of the two detectors are correlated, and then, we obtain the image. In order to demonstrate the feasibility of our scheme on the experiment and obtain a quantitative result, we take the methods of enhancing the index of refraction with EIT given by Ref. [20] as an example to discuss the following calculation. Since the refractive index is different for the two quasi-monochromatic beams (seen in Table 1), these two beams are separated in the space by propagating through the EIT media (seen in Fig. 2).

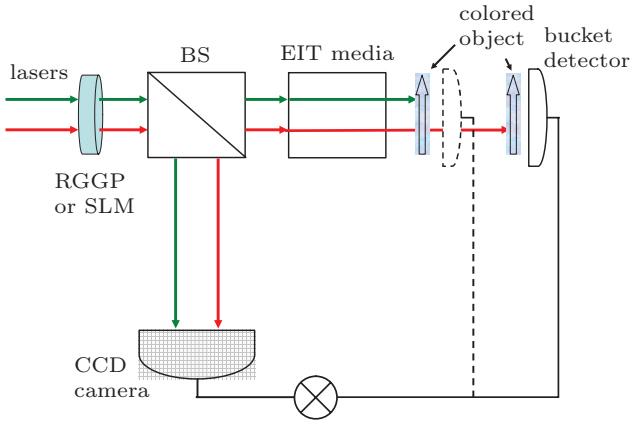


Fig. 1. (color online) Schematic diagram of ghost imaging with broad distance. RGGP: rotating ground glass plate; SLM: spatial light modulator; BS: beam splitter.

Table 1. The refractive index with vanishing absorption in high density vapor cells for different wavelengths. The EIT media is performed in a magnetically shielded, abundance potassium ($^{40}\mathrm{K}+^{39}\mathrm{K}$) vapor cell with a length of $L=1$ cm. The densities exceeding $N_{40\,\mathrm{K}}=10^{17}$ cm^{-3} and $N_{39\,\mathrm{K}}=10\,N_{40\,\mathrm{K}}$.

Wavelength/nm	532	770.1
Absorption	0	0
Refractive index	1	~5

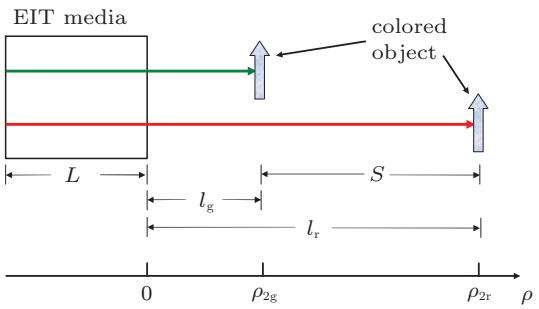


Fig. 2. (color online) The light beams are separated in signal arm by EIT media. L: the length of the EIT media. S: the effective broad distance of the GI. According to the above analysis, $S=5$ cm. l_r, l_g represent the distance between the object and the EIT media. ρ_{2r}, ρ_{2g} are corresponding to the coordinates in the signal arm.

The idler and signal light beams detected by the CCD camera and bucket detector can be expressed as[7,23]

$$E_{\eta,m}(\rho,t) = \begin{cases} \sqrt{\eta}\left(E_{\mathrm{ir}}(\rho,t)h_{\mathrm{r}}(\rho,\lambda_{\mathrm{r}})+E_{\mathrm{ig}}(\rho,t)h_{\mathrm{g}}(\rho,\lambda_{\mathrm{g}})\right), \\ \sqrt{\eta}T(\rho)\left(E_{\mathrm{sr}}(\rho,t)h_{\mathrm{r}}(\rho,\lambda_{\mathrm{r}})+E_{\mathrm{sg}}(\rho,t)h_{\mathrm{g}}(\rho,\lambda_{\mathrm{g}})\right), \end{cases} \quad (1)$$

where $E_{\mathrm{i}j}$ and $E_{\mathrm{s}j}$ represent the idler beam and signal fields, respectively; $j=$ r, g represents the red light and green light, respectively.

$$E_{mj}(\rho,t)=\int \mathrm{d}\omega\, \mathrm{e}^{-\mathrm{i}\omega t}\varepsilon_j(\omega) \quad (2)$$

is the quasi-monochromatic light fields, $m=$ i, s; the light fields are taken to be plane waves with spectra $\varepsilon_j(\omega)$.

$$h_j(\rho,\omega_j)=\frac{k\,\mathrm{e}^{\mathrm{i}k\left(l+|\rho|^2/2l\right)}}{\mathrm{i}2\pi l} \quad (3)$$

is the Huygens–Fresnel Green's function that describes propagation through the idler and signal arms, while $k=\omega_j/c$ is the wave number associated with the frequency ω. For simplicity, we assume that the CCD and bucket detector are two ideal detectors, i.e., no dark current and electronic thermal noise. The classical output currents from the bucket detector in the signal arm and CCD in the idler arm can be expressed as[23]

$$e_m(t) = q\int \mathrm{d}u \int_{A_n}\mathrm{d}\rho \times E^*_{\eta,m}(\rho,u)E_{\eta,m}(\rho,u)h_{\mathrm{B}}(t-u). \quad (4)$$

Here, q represents the electron charge; A low-pass filter with impulse response $h_{\mathrm{B}}(t)$ to model the real finite electrical bandwidth of the detector; $n=1,2$, A_1 and A_2 represent the photosensitive region of CCD and bucket detector, respectively.

The image is reconstructed by correlating the currents produced by the two detectors. Thus, we obtain

$$\begin{aligned} &\langle O(\rho_1)\rangle \\ &= \langle e_{\mathrm{i}}(t)e_{\mathrm{s}}(t)\rangle \\ &= q^2\eta^2 A_1\int_{A_2}\mathrm{d}\rho\int\mathrm{d}u_1\int\mathrm{d}u_2 h_{\mathrm{B}}(t-u_1)h_{\mathrm{B}}(t-u_2) \\ &\quad\times\left\langle E^*_{\eta,i}(\rho_1,u_1)E_{\eta,i}(\rho_1,u_1)E^*_{\eta,s}(\rho,u_2)E_{\eta,s}(\rho,u_2)\right\rangle. \end{aligned} \quad (5)$$

The idler and signal light beams obey the canonical commutation relations[23]

$$\begin{aligned} &\left[E_m(\rho_m,t_m)E_y(\rho_y,t_y)\right]=0, \\ &\left[E_m(\rho_m,t_m)E^*_y(\rho_y,t_y)\right]=\delta_{m,y}\delta(\rho_m-\rho_{\mathrm{g}})\delta(t_m-t_{\mathrm{g}}), \end{aligned} \quad (6)$$

where $m,y=$ (i, s); $\delta_{m,y}$ is a delta function; and $\delta(\cdots)$ is a unit impulse.

In order to obtain the expression of the ghost imaging, the commutator relation (4) is used to put the two fourth-order moments into normal order. Next, these two fourth-order moments are expressed in second-order moments by the Gaussian moment-factoring theorem.[24] Finally, the zero terms (i.e., phase-sensitive cross correlation) and background terms[24] are subtracted. The expression of the ghost imaging can be given by

$$\langle O(\rho_1)\rangle = q^2\eta^2 A_1 \int_{A_2} \mathrm{d}\rho \int \mathrm{d}u \int \mathrm{d}u h_{\mathrm{B}}(t-u_1)h_{\mathrm{B}}(t-u_2)\,|T(\rho)|^2\,\Delta\left\{|\langle E^*_{\mathrm{ir}}(\rho_1,u_1)E_{\mathrm{sr}}(\rho,u_2)\rangle|^2, \left|\langle E^*_{\mathrm{ig}}(\rho_1,u_1)E_{\mathrm{sg}}(\rho,u_2)\rangle\right|^2\right\}, \quad (7)$$

where $\Delta\{A,B\}$ represents either A or B and can be obtained simultaneously. In the thermal ghost imaging with degenerate-wavelength source, the RGGP is generally utilized to produce two correlated spatially incoherent light beams. In the thermal ghost imaging with a nondegenerate-wavelength source, this method is not suitable for creating spatial correlation between two light beams.[25] For a pseudothermal source, the phase-insensitive cross correlation has maximum value, given by[23]

$$\left\langle E^*_{\mathrm{i}j}(\rho_1,u_1)E_{\mathrm{s}j}(\rho_2,u_2)\right\rangle = \left(\frac{2P_j}{\pi a_0^2}\right)\mathrm{e}^{-(|\rho_1|^2+|\rho_2|^2)/a_0^2-|\rho_2-\rho_1|^2/2\rho_0^2}, \quad (8)$$

where $j=$ r, g; P represents the photon flux; a_0 represents the transverse intensity radius that is attenuated by e^{-2}, and ρ_0 represents the transverse coherence radius. The time factor and transfer function have been ignored in Eq. (8).[23] Thus, substituting Eq. (8) into Eq. (7), we obtain the broad distance thermal ghost imaging,

$$\langle O(\rho_1)\rangle = q^2\,\eta^2 A_1\left(\frac{2}{\pi a_0^2}\right)^2 \int_{A_2}\mathrm{d}\rho\,|T(\rho)|^2\,\mathrm{e}^{-2(|\rho_1|^2+|\rho|^2)/a_0^2-|\rho-\rho_1|^2/\rho_0^2}\Delta\left\{P_{\mathrm{r}}^2,P_{\mathrm{g}}^2\right\} = \Delta\left\{\left\langle O_{\mathrm{r}-\rho_{2\mathrm{r}}}(\rho_1)\right\rangle, \left\langle O_{\mathrm{g}-\rho_{2\mathrm{g}}}(\rho_1)\right\rangle\right\}, \quad (9)$$

where r, g, and ρ represent the color (red and green) of the ghost image and the coordinate of the object, respectively. Previous work shows that the imaging's spatial resolution of conventional ghost imaging is determined by the speckle's transverse size that is mainly determined by the numerical aperture.[17] The image obtained by this imaging is the same as the conventional ghost imaging,[23] thus, the spatial resolution of our imaging scheme is also determined by the numerical aperture. Generally, $l \gg \lambda$, thus, the change of spatial resolution arising from the different wavelength can be ignored.

It is noted that we cannot obtain two monochromatic ghost images at the same time (seen in Fig. 2). According to the color of GI,[26] only one monochromatic ghost image can be obtained based on the position of the object. Next, we will analyze it and obtain a very interesting and useful conclusion, i.e., the position (or distance) of the object can be ascertained by the color of the image. Thus, the imaging process and ranging process are combined together. We believe that this new GI scheme may be developed into a new ranging technique. According to Fig. 2, as the object is placed at the coordinate $\rho_{2\mathrm{r}}$, there is only the red light meeting the condition of generating the ghost image. Therefore, a red ghost image can be obtained.[26] Similarly, we can obtain a green ghost image when the object is placed at the coordinate $\rho_{2\mathrm{g}}$. In general, enhancing the index of refraction by EIT media is effective for a specific wavelength, e.g., Rb$\sim$780 nm, K$\sim$770.1 nm. However, the scope of the photonrefractive crystals (e.g., $BaTiO_3$, $LiNbO_3$, and $KNbO_3$) and dispersive crystals (e.g., SiO_2) covers the entire visible wavelengths. Thus, the coordinates may be approximated as it continuously changes when the light source with j ($j \gg 1$) wavelength is used. According to the above analysis, we obtain the length of the effective distance, i.e.,

$$S = (n_{\max} - n_{\min})L, \quad (10)$$

where $n_{\max}$ and $n_{\min}$ are the maximum refractive index and the minimum one of the optical media corresponding to the wavelengths involved in the ghost imaging, respectively.

More important, based on the above analysis, the position (or distance) of the object can be obtained by the image's color. We assume that the color of an image shows c-color. Thus, we obtain the distance between the object and the optical media, i.e.

$$l_{\mathrm{c}} = l_{\mathrm{idler}} - n_{\mathrm{c}}L, \quad (11)$$

where l_{idler} represents the length of the idler arm. Generally, it is difficult to merge the imaging process and ranging process together in a conventional optical imaging technique, because there is only the object (signal) light arm, not the reference (idler) light arm.

As the RGGP is replaced by the SLM, a monochromatic or full colored ghost image can be presented no matter what the object's position is. In this case, the operators appearing in the currents operators are the same as those in Eq. (4). However, previous works show that both degenerate wavelength spatial correlations and non-degenerate wavelength spatial correlations can be achieved by the SLM.[25,27] Thus, the imaging expression Eq. (7) is changed as

$$\begin{aligned}&\langle O(\rho_1)\rangle\\ &= q^2\eta^2 A_1\int_{A_2}\mathrm{d}\rho\int\mathrm{d}u_1\int\mathrm{d}u_2\\ &\times h_{\mathrm{B}}(t-u_1)h_{\mathrm{B}}(t-u_2)\,|T(\rho)|^2\\ &\times\Delta\left\{\left(|\langle E^*_{\mathrm{ir}}(\rho_1,u_1)E_{\mathrm{sr}}(\rho,u_2)\rangle|^2\right.\right.\\ &+\left.\left.\left|\langle E^*_{\mathrm{ig}}(\rho_1,u_1)E_{\mathrm{sr}}(\rho,u_2)\rangle\right|^2\right),\end{aligned}$$

$$\left(\left|\left\langle E_{\rm ig}^{*}(\rho_1,u_1)E_{\rm sg}(\rho,u_2)\right\rangle\right|^2 + \left|\left\langle E_{\rm ig}^{*}(\rho_1,u_1)E_{\rm sr}(\rho,u_2)\right\rangle\right|^2\right)\Big\}. \quad (12)$$

Here, the nondegerenate wavelength spatial correlations are given by[23]

$$\left\langle E_{ij}^{*}(\rho_1,u_1)E_{sw}(\rho_2,u_2)\right\rangle = \left(\frac{2P_{jw}}{\pi a_0^2}\right) {\rm e}^{-(|\rho_1|^2+|\rho_2|^2)/a_0^2-|\rho_2-\rho_1|^2/2\rho_0^2}, \quad (13)$$

where $j,w = {\rm r, g}$. Therefore, the broad distance ghost imaging with SLM can be expressed as

$$\begin{aligned}\langle O(\rho_1)\rangle &= q^2\eta^2 A_1\left(\frac{2}{\pi a_0^2}\right)^2\int_{A_2}{\rm d}\rho\,|T(\rho)|^2 \\ &\quad\times {\rm e}^{-2(|\rho_1|^2+|\rho|^2)/a_0^2-|\rho-\rho_1|^2/\rho_0^2} \\ &\quad\times \Delta\left\{\left(P_{\rm rr}^2+P_{\rm rg}^2\right),\left(P_{\rm gg}^2+P_{\rm gr}^2\right)\right\} \\ &= \Delta\left\{\left(\left\langle O_{{\rm rr}-\rho_{2\rm r}}(\rho_1)\right\rangle+\left\langle O_{{\rm rg}-\rho_{2\rm r}}(\rho_1)\right\rangle\right), \\ &\quad\left(\left\langle O_{{\rm gg}-\rho_{2\rm g}}(\rho_1)\right\rangle+\left\langle O_{{\rm gr}-\rho_{2\rm g}}(\rho_1)\right\rangle\right)\Big\}. \quad (14)\end{aligned}$$

Equation (14) shows that the image output from the coincidence measurements includes two sub-ghost images. One of the images comes from the degenerate wavelength spatial correlations (e.g., $\langle O_{{\rm rr}-\rho_{2\rm r}}(\rho_1)\rangle$, $\langle O_{{\rm gg}-\rho_{2\rm g}}(\rho_1)\rangle$), the other image comes from the nondegenerate wavelength spatial correlations (e.g., $\langle O_{{\rm rg}-\rho_{2\rm r}}(\rho_1)\rangle$ and $\langle O_{{\rm gr}-\rho_{2\rm g}}(\rho_1)\rangle$). According to previous work,[26] the two sub-ghost-images show two different colors, respectively. Ideally, the monochromatic laser has only one wavelength light, thus, the added ghost image is a monochromatic image because there is only a single wavelength light beam that interacts with the object. Consequently, we will obtain a monochromatic image regardless of where the object is. In practice, the laser beam is a quasi-monochromatic light, thus, the two quasi-monochromatic images will add together to form one colored image. As the EIT meida is replaced by a dispersive crystal, three or more wavelengths light beams (e.g., tricolor, i.e., red, green, and blue) can be used in the imaging. Therefore, a full colored image can be obtained.

The above analysis is based on the slow light technique. As we all know, there are other methods to obtain slow light except EIT. For instance, Rseidori *et al.* show that the slow and fast light can be obtained by the liquid crystal (532 nm).[21] Their work shows that the liquid crystal allows us to obtain ground velocities as slow as less than 0.2 mm/s. Therefore, the length of $S\sim$ kilometers. Thus, our scheme is suitable for space remote sensing that is the most attractive of GI in application.[17–19,28] It is noted that the 3D ghost imaging schemes proposed by Han *et al.*[17–19] have many advantages (e.g., high resolution, fast imaging), which is very useful in remote sensing. The advantages of our imaging scheme and Han's can be combined together, which promote the application of GI on remote sensing. Furthermore, our imaging scheme based on the dispersion can be applied to microscopy imaging. As the broad distance GI is achieved by photorefractive crystals or ordinary dispersive crystals, the ultra-high precision ranging can be achieved by the broad distance GI. We take the quartz as an example to illustrate this feature. The change of refractive index with wavelength is seen in Table 2.

Table 2. The refractive index with different wavelengths in quartz.

Wavelength/nm	410.2	546.1	766.5
Refractive index	1.5565	1.5462	1.5391

We assume that the thickness of the quartz plate is about 0.1 mm. Thus, our imaging scheme has a power of ranging and imaging the two objects between 1 μm, and appearing as two images with two different colors. Fortunately, this scale is exactly the size of the cells. Thence, our scheme has great potential in biological and medical imaging.

3. Conclusion

The ghost imaging with broad distance has been presented in this paper. We put an optical media at the signal arm. Thus, the signal light beams with different multiwavelegths are separated in space based on the dispersion principle. Meanwhile, the equality of the optical distance of the two light arms is not violated too. As the photon correlation is obtained by an RGGP, a monochromic ghost image can be obtained. According to this feature, the position (or distance) of the object can be ascertained by the color of the ghost image, which is very interesting and useful in application, because the imaging process and ranging process are combined together. As the RGGP is replaced by the SLM, we obtain a monochromic or colored image regardless of where the object is. Further studies of broad distance GI with continuous wave source will be considered in our future works. We hope that the new imaging scheme will pave the way to the application of GI in remote sensing, biological and medical imaging problems, and in particular, in the situations where conventional optical imaging appears not to be adequate, such as when the size of the object to be imaged is located in microscale.

References

[1] Cheng J and Lin J 2013 *Phys. Rev. A* **87** 043810
[2] Cheng J 2009 *Opt. Express* **17** 7916
[3] Meyers R E, Deacon K S and Shih Y 2010 *Appl. Phys. Lett.* **98** 111115
[4] Duan D Y, Zhang L and Xia Y J 2014 *J. Opt. Soc. Am. A* **31** 730
[5] Gong W L and Han S S 2011 *Opt. Lett.* **36** 394

[6] Bai Y F, Yang W X and Yu X Q 2012 *Chin. Phys. B* **21** 044206
[7] Duan D Y, Du S J and Xia Y J 2013 *Phys. Rev. A* **88** 053842
[8] Cheng J, Han S S and Yan Y J 2006 *Chin. Phys.* **15** 2002
[9] Zhang C, Gong W L and Han S S 2013 *Appl. Phys. Lett.* **102** 021111
[10] Luo C L and Cheng J 2013 *Opt. Lett.* **38** 5381
[11] Duan D Y, Zhang L, Du S J and Xia Y J 2015 *Chin. Phys.* **24** 024202
[12] Katz O, Bromberg Y and Silberberg Y 2009 *Appl. Phys. Lett.* **95** 131110
[13] Li M F, Zhang Y R, Luo K H, Wu L A and Fan H 2013 *Phys. Rev. A* **87** 033813
[14] Zhao S M and Zhuang P 2014 *Chin. Phys. B* **23** 054203
[15] Gong W L and Han S S 2012 *J. Opt. Soc. Am. A* **29** 1571
[16] Li M F, Zhang Y R, Liu X F, Yao X R, Luo K H, Fan H and Wu L A 2013 *Appl. Phys. Lett.* **103** 211119
[17] Zhao C Q, Gong W L, Chen M L, Li E R, Wang H, Xu W D and Han S S 2012 *Appl. Phys. Lett.* **101** 141123
[18] Gong W L and Han S S 2011 *Phys. Lett. A* **375** 990
[19] Li E R, Bo Z W, Chen M L, Gong W L and Han S S 2014 *Appl. Phys. Lett.* **104** 251120
[20] Simmons Z J, Proite N A, Miles J, Sikes D E and Yavuz D D 2012 *Phys. Rev. A* **85** 053810
[21] Residori S, Bortolozzo U and Huignard J P 2008 *Phys. Rev. Lett.* **100** 203603
[22] Lavoie B R, Leung P M and Sanders B C 2013 *Phys. Rev. A* **88** 023860
[23] Erkmen B I and Shapiro J H 2008 *Phys. Rev. A* **77** 043809
[24] Erkmen B I and Shapiro J H 2009 *Phys. Rev. A* **79** 023833
[25] Chan K W C, O'Sullivan M N and Boyd R W 2009 *Phys. Rev. A* **79** 033808
[26] Duan D Y, Du S J, Yan L, Jiang S S, Liu Y Y, Zhang L and Xia Y J 2014 *Eur. Phys. J. D* **68** 11
[27] Shapiro J H, Venkatraman D and Wong N F C 2013 *Sci. Rep.* **3** 1849
[28] Wang C F, Zhang D W, Bai Y F and Chen C 2010 *Phys. Rev. A* **82** 063814